Characterization of Metabolism in the Fe(III)-Reducing Organism *Geobacter sulfurreducens* by Constraint-Based Modeling†

R. Mahadevan,[1]* D. R. Bond,[2]‡ J. E. Butler,[2] A. Esteve-Nuñez,[2] M. V. Coppi,[2]
B. O. Palsson,[1] C. H. Schilling,[1] and D. R. Lovley[2]

*Genomatica, San Diego, California 92121,[1] and Department of Microbiology,
University of Massachusetts, Amherst, Massachusetts 01003[2]*

Geobacter sulfurreducens **is a well-studied representative of the** *Geobacteraceae*, **which play a critical role in organic matter oxidation coupled to Fe(III) reduction, bioremediation of groundwater contaminated with organics or metals, and electricity production from waste organic matter. In order to investigate** *G. sulfurreducens* **central metabolism and electron transport, a metabolic model which integrated genome-based predictions with available genetic and physiological data was developed via the constraint-based modeling approach. Evaluation of the rates of proton production and consumption in the extracellular and cytoplasmic compartments revealed that energy conservation with extracellular electron acceptors, such as Fe(III), was limited relative to that associated with intracellular acceptors. This limitation was attributed to lack of cytoplasmic proton consumption during reduction of extracellular electron acceptors. Model-based analysis of the metabolic cost of producing an extracellular electron shuttle to promote electron transfer to insoluble Fe(III) oxides demonstrated why** *Geobacter* **species, which do not produce shuttles, have an energetic advantage over shuttle-producing Fe(III) reducers in subsurface environments. In silico analysis also revealed that the metabolic network of** *G. sulfurreducens* **could synthesize amino acids more efficiently than that of** *Escherichia coli* **due to the presence of a pyruvate-ferredoxin oxidoreductase, which catalyzes synthesis of pyruvate from acetate and carbon dioxide in a single step. In silico phenotypic analysis of deletion mutants demonstrated the capability of the model to explore the flexibility of** *G. sulfurreducens* **central metabolism and correctly predict mutant phenotypes. These results demonstrate that iterative modeling coupled with experimentation can accelerate the understanding of the physiology of poorly studied but environmentally relevant organisms and may help optimize their practical applications.**

Geobacter species were the first organisms found to have the ability to conserve energy for growth by completely oxidizing organic compounds to carbon dioxide with Fe(III) serving as the electron acceptor (12, 57, 58). *Geobacter* species can play an important role in organic matter oxidation in both pristine and contaminated subsurface environments (2, 55, 56, 88). In addition to transferring electrons to Fe(III), *Geobacter* species can also reduce a variety of toxic and radioactive metals (51, 52, 59, 70). Moreover, stimulating the activity of *Geobacter* species in the subsurface is an effective strategy for removing such contaminants from groundwater (3, 41, 55). Another practical application of *Geobacter* species is derived from their ability to oxidize organic compounds with an electrode serving as the electron acceptor (8, 9, 41), which makes it possible to harvest electricity from waste organic matter.

The metabolism of *Geobacter* species has not been studied in detail. It is clear that their metabolism differs from the anaerobic metabolism of several well-studied organisms, such as *Escherichia coli*, that rely primarily on sugar fermentation to produce energy and biosynthetic precursors. In *Geobacter*, ac-

etate and other electron donors are completely oxidized via the tricarboxylic acid (TCA) cycle (14, 34), necessitating electron transfer to terminal electron acceptors for the regeneration of cytoplasmic and intramembrane electron acceptors and ATP synthesis. Furthermore, the need to transfer electrons to extracellular electron acceptors, such as Fe(III) oxides, poses biochemical challenges not faced during microbial reduction of soluble electron acceptors that can be reduced within the cell (58, 80).

The complete genome of *Geobacter sulfurreducens* was recently sequenced, providing insights into the physiological properties of *Geobacter* species (54, 62), including the elucidation of novel adaptive strategies such as Fe(II)-based chemotaxis (15) and the previously unsuspected ability to respire oxygen (48). However, it is not possible to predict the physiology of *G. sulfurreducens* from the annotated sequence alone.

The constraint-based approach to modeling microbial metabolism, which does not require detailed kinetic parameters for individual metabolic reactions, has proven to be an effective strategy for predicting the physiological responses of microorganisms (44, 77, 87). This approach relies on implementing a series of physicochemical constraints, including thermodynamic directionality, and enzymatic capacity constraints and reaction stoichiometry constraints arising from the requirement that fluxes consuming and producing both metabolites and protons are balanced. To date, this method has been primarily applied to well-studied microorganisms and patho-

* Corresponding author. Mailing address: Genomatica, 5405 Morehouse Dr., Ste. 210, San Diego, CA 92121. Phone: (858) 362-8562. Fax: (858) 824-1772. E-mail: rmahadevan@genomatica.com.
† Supplemental material for this article may be found at http://aem.asm.org/.
‡ Present address: BioTechnology Institute and Department of Microbiology, University of Minnesota, St. Paul, MN 55108.

gens such as *E. coli* (26, 27, 79), *Saccharomyces cerevisiae* (24, 30), *Haemophilus influenzae* (25), and *Helicobacter pylori* (82).

Here we describe the application of the constraint-based modeling approach, coupled in an iterative fashion with experimental studies, to further elucidate the physiology of *G. sulfurreducens*. The results demonstrate that this approach can accelerate discovery as well as provide insights into the ecology of *Geobacter* species, by enabling the exploration of metabolic responses to a variety of genetic and environmental perturbations, thereby generating testable hypotheses.

MATERIALS AND METHODS

Metabolic network reconstruction. The *G. sulfurreducens* metabolic network was reconstructed from open reading frames (ORFs) encoded in the *G. sulfurreducens* genome (62) by using previously described metabolic reconstruction procedures and available metabolic databases (21, 37, 43, 71). Metabolic functions were assigned to the genes in the *G. sulfurreducens* genome (62) based on available biochemical and genetic evidence (20, 34) and sequence similarity. Every gene reaction association included in the network was assigned a confidence score based on the level of sequence similarity (a BLAST value of <1e-20 was assigned a high score) to homologous biochemically or genetically characterized genes and the availability of biochemical and genetic evidence. In some instances, genes for biosynthetic reactions known to be necessary to support growth could not be identified, and these reactions (55 reactions) were added to the network without being assigned to specific genes.

The SimPheny (Genomatica, San Diego, CA) platform was used to create and curate the current reconstruction. All of the reactions incorporated into the network were elementally and charge balanced and included information on the localization (cytoplasmic or extracellular) of the reactants and products. Charges on all metabolites were calculated assuming a physiological pH (intracellular) of 7.4 by using Pipeline Pilot (Scitegic, San Diego, CA).

Strain and culture conditions. Wild-type *G. sulfurreducens* (ATCC 51573) and the FrdA-knockout strain (11) were obtained from our laboratory collection. *G. sulfurreducens* was grown in batch and continuous culture in two defined, bicarbonate-buffered mineral media, i.e., freshwater acetate-fumarate medium (5.5 mM:30 mM) and acetate-Fe(III) citrate medium (5.5 mM:55 mM), under strict anaerobic conditions at 30°C using previously described methods (28, 29). Cell growth was monitored by determining total protein by the bicinchoninic acid method with bovine serum albumin as a standard (85), and organic acid production was monitored by high-performance liquid chromatography (HPLC) as previously described (28).

Determination of biomass composition. Cultures for biomass composition determinations were grown in acetate-fumarate medium, harvested in exponential phase ($\mu \sim 0.1$ h^{-1}) when cultures were at half-maximal optical density, and resuspended in deionized water. Dry weight was determined gravimetrically after drying at 105°C for 24 h. Lipids (32), DNA, and RNA were analyzed as previously described (39, 83). The carbohydrate weight fraction was estimated by the anthrone method, with glucose as a standard (4). The weight fractions of the various macromolecules were calculated to be as follows: protein (46%), RNA (10%), DNA (4%), lipids (15%), and total carbohydrate (15%). The remainder of the biomass was assumed to consist of lipopolysaccharides (4%), peptidoglycan (4%), and ions (2%). The distribution of the amino acids, nucleotides, lipopolysaccharides, and ions in the biomass was assumed to be similar to that of *E. coli* (64, 65). The detailed lipid composition was assumed to be similar to that of *G. metallireducens* (57).

The biomass composition described above was used to create a reaction in the network reconstruction that represented growth-associated biosynthetic demands and was used in all simulations (reaction name agg_GS13m [see Tables S1 and S2 in the supplemental material]). This reaction includes energetic requirements, as well as cytoplasmic proton generation associated with the formation of peptide bonds and other biomass components.

In silico analysis of metabolism. A genome-scale metabolic model for *G. sulfurreducens* was developed by using the constraint-based modeling approach (7, 44, 87) and the SimPheny (Genomatica, San Diego, CA) platform. For growth simulations, the objective of maximization was the production of biomass. Some combinations of transport reactions in the metabolic model could exchange protons across the membrane, effectively constituting a proton pump without energetic requirements. Such violations of thermodynamic considerations were prevented by constraining the corresponding reactions such that they were consistent with electrochemical and ion gradients commonly known to exist

in bacteria (5, 76). The complete list of genes, reactions, metabolites, applied constraints, and confidence scores is available online (http://www.geobacter.org/) and in Table S1 in the supplemental material.

The stoichiometry associated with the list of metabolic reactions, along with the directionality constraints, and the substrate uptake rates corresponding to the environmental variables (media conditions) were used to define the constraints on the fluxes (reaction rates) based on the assumption that fluxes producing and consuming a metabolite are balanced at steady state. These constraints define the solution boundary in the metabolic flux space, and a single metabolic flux distribution that maximized a "cellular objective" was calculated through linear optimization. The linear programming problem was solved in SimPheny using the revised Simplex solver from Lindo (Lindo Systems, Inc., Chicago, IL). The initial point for the Simplex algorithm was not explicitly specified in the formulation and was assumed to be the default value determined by the algorithm. This algorithm identifies a single point that is optimal even though there can be multiple points (i.e., an edge) that are optimal. For details, the interested reader is referred to the cited book by Chvatal (16). It has been established that these alternate optimal solutions have the same objective value (i.e., growth rate when it is selected for maximization) but different metabolic flux distributions due to redundancies in the metabolic pathways (46, 61). Typically, only one of the alternate optimal solutions, in which a specific redundant pathway is active, is identified by the linear programming algorithm. In addition, there are reactions ("blocked reactions") in incomplete pathways that are never predicted to be active under any condition and conditionally active reactions that are active only under specific environments. The details on the computation and the interpretation of these blocked reactions and redundant pathways are presented elsewhere (10, 61).

For all simulations presented here, all genes included in the network were assumed to be expressed and their associated reactions were assumed to be functional. Maximization of biomass production (growth) was the objective for all of the simulations except for the comparison of amino acid synthesis capabilities. In silico deletion analysis was performed by eliminating specific genes and their associated reactions from the model. For analysis of the energetics of menaquinone secretion, an additional menaquinone secretion rate constraint was incorporated.

RESULTS AND DISCUSSION

Metabolic network reconstruction. BLAST (1) searches of publicly available databases (21, 37, 43, 71) resulted in the identification of 588 genes that could be associated with 467 distinct metabolic reactions. These reactions were further refined by using published biochemical and physiological information (e.g., preference of isocitrate dehydrogenase for NADP$^+$ versus NAD$^+$, etc.) (13, 14, 34, 35, 72, 91). To allow full stoichiometric balancing, all reactions were entered into the model database as balanced reactions, including the net charge of each metabolite or cofactor and the localization (cytoplasmic or extracellular) of reactants and products. Reactions causing futile or thermodynamically infeasible cycles were constrained (76). However, if there was no strong evidence limiting the direction or magnitude of flux through a specific reaction, then metabolic reactions were allowed infinite flux in either direction.

Identification and closure of network gaps. The initial database was used to construct a preliminary metabolic model for *G. sulfurreducens*, and simulations were performed to determine whether this collection of independent reactions could synthesize a full complement of DNA, RNA, amino acids, lipids, carbohydrates, and cofactors from acetate and a defined mineral medium containing vitamins (29). These simulations revealed gaps in the network that required additional evaluation. For example, *G. sulfurreducens* is typically cultured with ammonia as the sole nitrogen source, and yet the network was unable to synthesize lysine, serine, alanine, and threonine. Synthesis of lysine by the network necessitated the incorporation

of two non-gene-associated reactions (tetrahydropicolinate succinylase and succinyl-diaminopimelate desuccinylase) to allow production of the key metabolite meso-2,6-diaminopimelate from 2,3,4,5-tetrahydrodipicolinate.

In order to close gaps detected in the network and enable synthesis of all growth precursors, a total of 55 non-gene-associated reactions were added. These included reactions to complete menaquinone and fatty acid biosynthesis and allow exchange of diffusible metabolites and gases (e.g., diffusion of H_2, N_2, and CO_2), as well as those required for amino acid biosynthesis. A list of these non-gene-associated reactions is presented in Table S3 in the supplemental material. However, even after the addition of these reactions, there were network gaps in poorly characterized biochemical pathways. Reactions in such pathways (denoted as blocked reactions) were predicted to be inactive in all model simulations even though they were incorporated into the model (10).

Previous analysis of the *G. sulfurreducens* genome suggested the potential for ammonia oxidation and autotrophic growth on one-carbon compounds (62). However, the pathways for these two types of metabolism appeared to be incomplete. Furthermore, there is no physiological evidence that *G. sulfurreducens* can grow with NH_4 as an electron donor or grow in the absence of an additional carbon source if either formate or H_2 is provided as the electron donor (12). Therefore, reactions that would lead to completion of the pathways for autotrophic growth and ammonia oxidation were not incorporated into the model.

The completed reconstructed metabolic network of *G. sulfurreducens* contained 588 genes (or 17% of a total of 3,467 ORFs), 522 biochemical reactions, and 541 unique metabolites. A full list of all gene-associated reactions is provided in Table S1 in the supplemental material.

Evaluation of the proton translocation stoichiometry during fumarate reduction. Once a network capable of synthesizing biomass in minimal medium under standard conditions was constructed, unique aspects of *Geobacter* energy metabolism and physiology were integrated. The reactions in the model included explicit details of proton production and the movement of protons between the cytoplasmic and extracellular compartments. Hence, the model provided a unique platform for evaluating mechanisms of energy generation. This characteristic was especially advantageous for studying *Geobacter* species, which are completely dependent upon electrogenic electron transport for ATP production and cannot generate ATP from acetate via substrate-level phosphorylation (58).

Fumarate reduction was selected as the first energy generation mode to be examined with the metabolic model. Extensive literature is available regarding microbial fumarate respiration, and fumarate, in contrast to extracellular electron acceptors typically exploited by *Geobacter* species, is an intracellular electron acceptor involving a relatively simple electron transport chain (18). In addition, experimental observations of growth in the presence of fumarate indicate that *G. sulfurreducens* can neither oxidize fumarate nor utilize fumarate as a carbon or energy source, even when grown in the presence of noncarbon electron donors such as hydrogen (12, 19, 29, 34).

Genetic studies indicate that *G. sulfurreducens* utilizes a single, three-subunit membrane-bound complex (FrdABC) with a cytoplasmic active site for both the reduction of fumarate and

the oxidation of succinate (11). The bifunctional fumarate reductase/succinate dehydrogenase of *G. sulfurreducens* is homologous to the characterized, di-heme, menaquinone-reducing succinate dehydrogenase of *Bacillus subtilis* and the menaquinone-oxidizing fumarate reductases of *Wolinella succinogenes* and belongs to heterotrimeric B-type family of fumarate reductases and succinate dehydrogenases (11, 38). During fumarate reduction by *G. sulfurreducens*, the succinate dehydrogenase is not required for fumarate production, since fumarate is present in the media and the TCA cycle operates as an "open loop" (11, 34). Therefore, only six electrons, in the form of NADH, NADPH, and ferredoxin, are derived from oxidation of acetate during fumarate reduction with the fumarate reductase serving as the terminal electron accepting step.

In the metabolic model, all reducing equivalents derived from the TCA cycle were assumed to be interconverted to NADH and enter the menaquinone pool via the two 14-subunit type I NADH dehydrogenase complexes that are encoded in the *G. sulfurreducens* genome (62). Type I NADH dehydrogenases typically translocate at least two charge equivalents per NADH oxidized and catalyze the consumption of two cytoplasmic protons during menaquinone reduction (33, 89). Whether menaquinol oxidation results in electrogenic translocation at the fumarate reductase was less clear. The succinate dehydrogenase of *B. subtilis* has been suggested to be electrogenic (84). However, more recent biochemical evidence indicates that the fumarate reductases of *W. succinogenes*, *Rhodothermus marinus*, and *B. subtilis* are not electrogenic (6, 31, 36, 45). Thus, three possible mechanisms for generating energy during growth with fumarate were examined: translocation at both the NADH dehydrogenase and the fumarate reductase, translocation at the NADH dehydrogenase alone, and translocation only by fumarate reductase. Simulations were performed assuming an H^+/ATP ratio of 4.

Only one of these scenarios, in which proton translocation occurred at the NADH dehydrogenase alone, was consistent with both thermodynamic considerations and available experimental data. The lower boundary for the $\Delta G'$ of acetate oxidation coupled to fumarate reduction was calculated to be approximately -186 kJ/mol acetate, based on the steady-state concentrations of substrates and products present in the medium during acetate-limited growth in chemostats ($\mu \sim 0.05$ h^{-1}) (29). Given a $\Delta G'$ for ATP synthesis of -60 kJ/mol (47), a maximum of 3 mol of ATP synthesized/mol of acetate oxidized was estimated. If the NADH dehydrogenase was considered to be the sole electrogenic site, then the maximum electron transport stoichiometry was $2H^+$/$2e^-$, where ne^- is the number of electrons, and a total of 1.5 mol of ATP could be generated per mol of acetate, a value well within the thermodynamic boundary of 3 mol of ATP per mol of acetate established above. If both NADH dehydrogenase and fumarate reductase were electrogenic, the electron transport stoichiometry increased to $4H^+$/$2e^-$, resulting in 3 mol of ATP/mol of acetate, which was at the thermodynamic boundary, and hence unlikely to occur in vivo. Translocation at the fumarate reductase alone was excluded based on the observation that growth yields per mole of succinate produced were similar during growth with acetate and that with hydrogen (19). If the fumarate reductase operated as an electrogenic redox loop, hydrogen oxidation would result in translocation of $4H^+$/$2e^-$ versus

$2H^+/2e^-$ for acetate oxidation, which would manifest as a significantly higher growth yield per electron.

Evaluation of the proton translocation stoichiometry during Fe(III) reduction. Analysis of the in silico growth of *G. sulfurreducens* under Fe(III)-reducing conditions uncovered an important energetic dilemma facing Fe(III)-reducing bacteria. To adapt the model of fumarate reduction to Fe(III) reduction, Fe(III) reduction was first modeled as a reaction that occurred outside the cell, consistent with numerous experimental observations (18) and the fact that insoluble Fe(III) oxides are the predominant form of Fe(III) in most soils and sediments (53). Under Fe(III)-reducing conditions, the TCA cycle operated as a closed loop (34) and produced eight electrons per mole of acetate oxidized. Menaquinone reduction was considered to occur as a consequence of a nonelectrogenic succinate dehydrogenase and a proton-pumping NADH dehydrogenase as described for fumarate reduction, resulting in the translocation of six H^+ per acetate oxidized. However, model simulations using this electron transport scheme indicated that cells would not be capable of growth (in silico) under Fe(III)-reducing conditions.

The inability of a single $2H^+/2e^-$ NADH dehydrogenase coupling site to support simulated Fe(III)-dependent growth was traced to the fact that the site of Fe(III) reduction was extracellular. The eight cytoplasmic protons that were produced from each mole of acetate oxidized in the cytoplasm were consumed in the cytoplasm when fumarate was the electron acceptor. In contrast, during Fe(III) reduction, electrons were transported outside the cell, while leaving protons in the cytoplasm, effectively dissipating the membrane potential and acidifying the cytoplasm. In order to generate sufficient energy to compensate for the production of protons in the cytoplasm, an additional coupling step was required.

The most likely mechanism for additional membrane potential generation during Fe(III) reduction was during transfer of electrons into the periplasmic cytochrome pool. Based on the fact that cytochromes implicated in Fe(III) reduction have midpoint potentials in the range of -190 mV (*omcB*) (60) and -136 to -155 mV (*ppcA*) (50), the energy available for coupling at this site could support translocation of $1H^+/2e^-$. This reaction was modeled as the release of menaquinol protons back to the cytoplasm by a protein capable of translocating 1 H^+ per pair of electrons transferred to the cytochrome pool. Inclusion of this reaction and accounting for all of the protons produced and consumed during metabolism resulted in a theoretical maximum yield with Fe(III) as the electron acceptor of 0.5 mol of ATP/mol of acetate compared to the 1.5 mol of ATP/mol of acetate during fumarate reduction. This output of the model provides an explanation for the experimental finding that growth yields of *G. sulfurreducens* are ~3-fold higher when fumarate serves as the terminal electron acceptor than during growth with Fe(III)-citrate (29). This experimental result was initially surprising because it is not consistent with expectations based on available energy, since the mid-point potential of the fumarate-succinate redox couple (at pH 7) is 0.03 V, whereas that of the Fe(III)-citrate/Fe(II) couple is 0.37 V.

These results suggest that reducing extracellular electron acceptors such as Fe(III) oxides, Fe(III)-citrate, elemental sulfur (S°), or electrodes will result in the generation of less biomass per electron transferred than growth with intracellu-

larly reduced electron acceptors. This may be an important consideration for applications such as bioremediation and electricity harvesting from waste organic matter, in which electron transfer to metals or electrodes, rather than production of biomass, is the primary goal.

Incorporation of physiological parameters. Once the proton translocation stoichiometry was determined, the next step in the development of the model was incorporation of physiological parameters, namely, the biomass component demands and maintenance energy requirements. First, a reaction representing growth-associated biosynthetic demands was constructed based on measurements of *G. sulfurreducens* biomass composition (see Materials and Methods). This reaction takes into account the amounts of 58 metabolites, cofactors, precursors, and ions required to synthesize each gram (dry weight) (gdw) of biomass, as well as proton consumption for reductive reactions, and the calculated ATP costs for the polymerization (peptide bond formation, DNA replication, and RNA polymerization) and biosynthesis of precursors and metabolites (see Table S2 in the supplemental material).

The ATP demand due to non-growth-associated energy functions, such as maintenance of ion gradients, turnover of RNA, and regulatory metabolism, was estimated by plotting acetate consumption during acetate-limited growth in chemostats with fumarate serving as the electron acceptor versus growth rate, extrapolating acetate consumption at a growth rate of zero (66, 73), and calculating the amount of ATP that would be produced from oxidation of this amount of acetate. This flux (ATPM: 0.45 mmol of ATP/gdw/h) was then used in conjunction with the biomass demand equation to predict the in silico growth yield of *G. sulfurreducens* over a range of growth rates. Comparison of these predictions with chemostat-derived growth yields (29) indicated that an additional flux of 46.7 mmol of ATP/gdw was consumed for growth-associated energy demands. This value was included as part of the biomass synthesis equation for all further growth simulations.

Evaluating model robustness. The metabolic reaction network, combined with demand reactions for biomass synthesis, correctly predicted growth yields and acetate consumption rates for growth in standard acetate-limited chemostats ($\mu = 0.06$ h^{-1}) with Fe(III)-citrate or fumarate as the electron acceptor (Fig. 1). Perturbations in variables used to construct the model, such as the biomass composition, which was derived from batch cultures of fumarate grown cells, had minimal effect on predicted growth yields for *G. sulfurreducens*. For instance, when a range of biomass composition equations (e.g., reflecting a range from 0.4 to 0.55 g of protein/gdw) were incorporated into the model, predicted yields were not significantly affected (1.5 to 2.5% differences). By comparison, a change in electron acceptor from fumarate to Fe(III) citrate caused threefold differences in yield or respiration rates (29). This revealed that the model predictions were robust to changes in biomass composition and nutrient availability, which was consistent with other work showing that variations in biomass composition produce only subtle effects on predicted growth yields or fluxes through central metabolic pathways (23, 74, 75). Hence, it is possible to assume that even significant changes (10 to 20%) in biomass composition would not affect the nature of metabolic predictions.
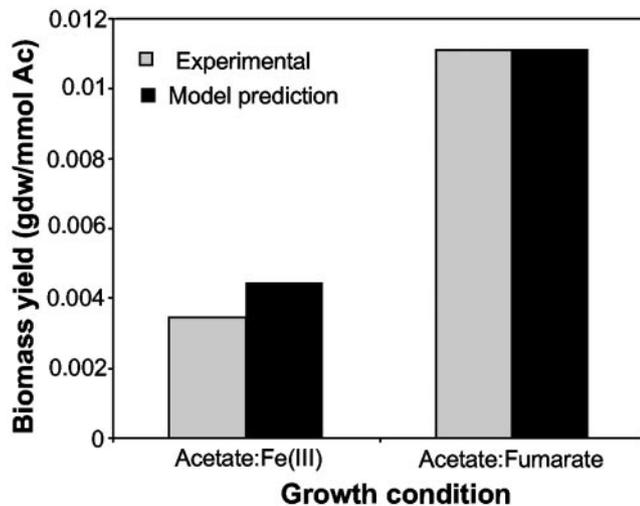
FIG. 1. Comparison of the biomass yields predicted by the in silico model with experimental data (29) derived from growth in chemostats under acetate-limiting conditions (5.5 mM acetate and 30 mM fumarate) at a rate of 0.06 h^{-1}. Model simulations of acetate-limited growth were carried out by constraining the growth rate at 0.06 h^{-1} and minimizing the acetate uptake rate. Variability in model predictions due to changes in biomass composition was estimated to be less than 5%.

Model-based characterization of *G. sulfurreducens* metabolism. Examination of the reconstructed metabolic network revealed that *G. sulfurreducens* has multiple pathways for acetate utilization (acetyl-coenzyme A [acetyl-CoA] transferase, acetate kinase, and phosphotransacetylase), interconversion of pyruvate to acetyl-CoA (pyruvate formate lyase, pyruvate

ferredoxin oxidoreductase, and pyruvate dehydrogenase), and anapleurotic reactions (phosphoenolpyruvate [PEP] carboxykinase and pyruvate carboxylase). Simulations predicted that during acetate-limited growth with Fe(III)-citrate (acetate uptake rate of 13.63 mmol/gdw/h for a growth rate of 0.06 h^{-1}), 93.6% of all acetate transported into the cell was utilized for oxidation and ATP generation via the TCA cycle (as flux through citrate synthase, or 12.76 mmol/gdw/h [Fig. 2]).

Flux from acetyl-CoA to pyruvate via pyruvate-ferredoxin oxidoreductase was predicted to be the sole source of carbon fixation in *G. sulfurreducens*, and in silico, 4% of consumed acetate (0.55 mmol/gdw/h) was utilized in this fixation reaction when Fe(III)-citrate was the electron acceptor. These values compared favorably with radiolabeling experiments in a close marine relative of *G. sulfurreducens*, *Desulfuromonas acetoxidans*, in which acetate oxidation linked to reduction of extracellular sulfur resulted in 4% of acetate being fixed into cell carbon via a labeling pattern consistent with the use of pyruvate ferredoxin oxidoreductase (35).

Activation of acetate via acetyl-CoA transferase only provided acetyl-CoA at a rate equal to the flux through the TCA cycle due to the dual role of the transferase in completing the TCA cycle (succinate to succinyl-CoA) and activating acetate. Thus, flux through an additional acetate activation pathway (acetate kinase [0.94 mmol/gdw/h]) was required to provide sufficient acetyl-CoA for pyruvate synthesis to meet gluconeogenic and anapleurotic demands. The major demand for pyruvate (54%) in *G. sulfurreducens* was predicted to be PEP synthesis for gluconeogenic reactions. Activation of pyruvate to PEP consumed 5.1% of the ATP flux in the cell, a value that doubled if the cost of activating acetate to acetyl-phosphate was considered. These distributions indicated that the avail-
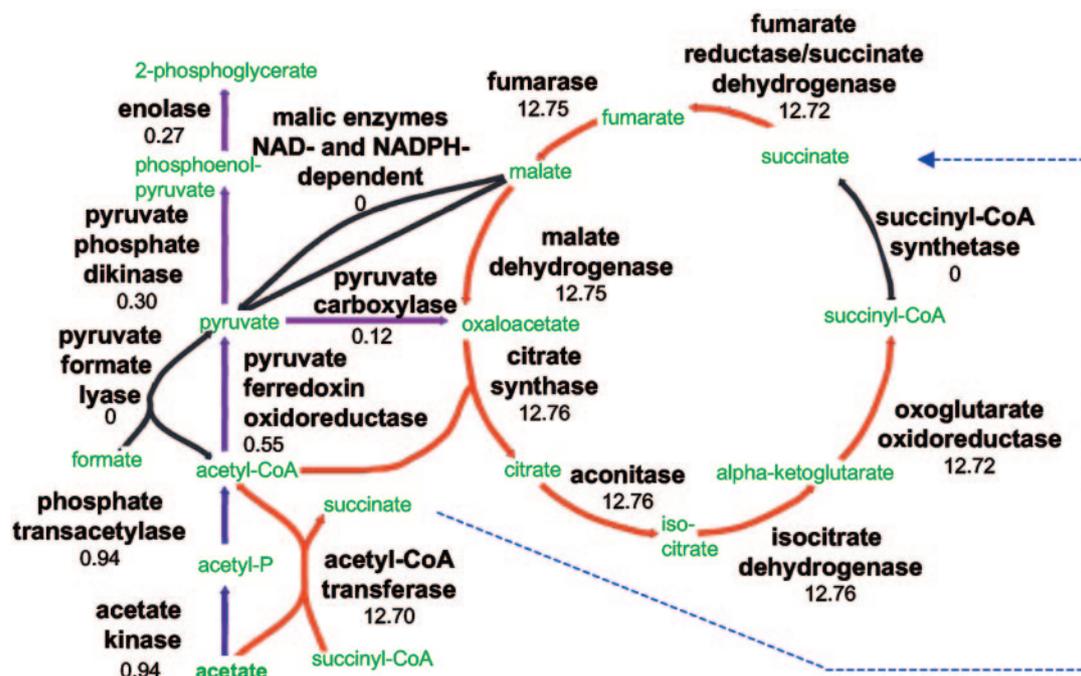

FIG. 2. Predicted flux distribution through central metabolism in *G. sulfurreducens* during in silico growth with limiting acetate and excess Fe(III)-citrate (growth rate of 0.06 h^{-1}). Red arrows indicate reactions with the greatest flux, and blue arrows indicate reactions with the least flux. Black lines indicate pathways with no associated flux. Flux predictions (in mmol/gdw/h) are listed below enzyme names.

ability of exogenous compounds with three or more carbons would eliminate this significant acetate and ATP demand and demonstrated the metabolic specializations which enable *G. sulfurreducens* to use acetate as both a carbon source and electron donor.

Although a complete pathway for glycolysis could be reconstructed, there is no physiological evidence that *G. sulfurreducens* can grow with glucose as an electron donor (12). This is most likely due to the fact that no sugar transporters appear to be present in the genome of *G. sulfurreducens*. Incorporation of the appropriate transporters into the model suggested that *G. sulfurreducens* could be genetically engineered to grow not only on glucose but also on substrates such as threonine, malate, and glycerol. This possibility is currently under experimental investigation.

As described above, *G. sulfurreducens* can neither oxidize fumarate for the production of energy nor utilize fumarate as a carbon source (12, 19, 34). The only potential fumarate transporter that could be conclusively identified in the *G. sulfurreducens* genome was a homolog of the dicarboxylate exchanger of *Wolinella succinogenes* (86), which can catalyze the exchange of fumarate and succinate (DcuB encoded by GSU2751). This gene is absent from the genome of a closely related species, *G. metallireducens*, which cannot grow with fumarate as an electron acceptor. Expression of *G. sulfurreducens* DcuB in *G. metallireducens* renders it capable of exploiting fumarate as an electron acceptor, suggesting that DcuB is indeed involved in fumarate uptake (11). Model simulations with DcuB as the only route of fumarate entry indicated that a possible explanation for the inability of *G. sulfurreducens* to assimilate fumarate as a carbon source is the requirement for equimolar succinate secretion by the exchanger in order to allow fumarate uptake. Since these results appear to be consistent with experimental data, the only mode of fumarate uptake that was incorporated into the model was this dicarboxylate exchanger.

Comparisons of amino acid synthesis by *G. sulfurreducens* and *E. coli* metabolic networks. The abilities of the *E. coli* (iJR904) (79) and *G. sulfurreducens* metabolic networks to synthesize amino acids with acetate serving as the sole carbon source and electron donor were compared. The reactions associated with Fe(III) reduction in the in silico model of *G. sulfurreducens* were incorporated into the *E. coli* model. The ATP maintenance parameters and the electron transport chain in *E. coli* were replaced with the corresponding parameters and reactions from *G. sulfurreducens* in order to isolate the role of central metabolism and eliminate the effect of differences in electron transport on the ability to synthesize amino acids. The amino acid production rate was maximized for each individual amino acid at a fixed acetate uptake rate of 10 mmol/gdw/h. By analyzing the differences in the predicted yields under identical growth conditions, it was possible to detect differences in the metabolic capabilities of the two networks and explore the sources of any disparities. One key difference found during the present study was that the metabolic network of *G. sulfurreducens* was more efficient at synthesizing most amino acids when acetate was the electron donor (Fig. 3, efficiency determined as moles of amino acid synthesized per mole of acetate consumed). This discrepancy was not due to differences in the amino acid biosynthetic pathways themselves and was most
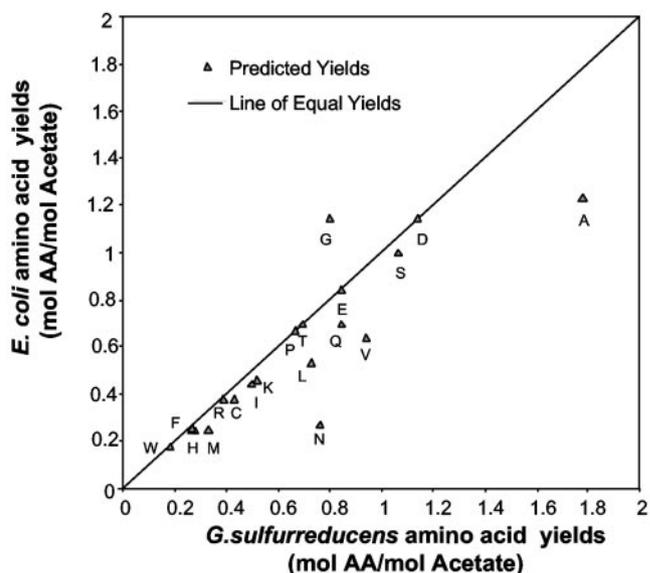

FIG. 3. In silico comparison of maximum amino acid yields per mol of acetate for the *G. sulfurreducens* and *E. coli* metabolic networks under acetate-limiting conditions with Fe(III) as the electron acceptor. The *E. coli* network (79) was modified to have an electron transport chain identical to that of *G. sulfurreducens*. Acetate uptake rate was constrained to 10 mmol/gdw/h.

dramatic in amino acids belonging to the pyruvate and aspartate families.

The key reaction that accounted for these differences was the production of 3-carbon units from activated acetate. In the case of *G. sulfurreducens*, pyruvate ferredoxin oxidoreductase catalyzed the synthesis of pyruvate from one molecule each of acetyl-CoA and CO_2, whereas in *E. coli* pyruvate synthesis required the use of the glyoxalate bypass in which 2 moles of acetyl-CoA are consumed and 1 mole of CO_2 is produced (22). Interestingly, incorporating this key reaction along with reactions enabling production of ferredoxin into the *E. coli* network led to amino acid yields equal to those of *G. sulfurreducens*. These simulations illustrate how metabolism in *G. sulfurreducens* is adapted for acetate utilization and how growth with acetate can be selective for the presence of pathways that fix carbon dioxide compared to selection for growth with larger carbon compounds that reduce carbon fixation demands.

Analysis of the metabolic cost of extracellular quinones. It has been hypothesized that one reason why *Geobacter* species predominate over other Fe(III)-reducing microorganisms in many subsurface environments is that *Geobacter* species expend less energy to reduce Fe(III) oxides than other Fe(III)-reducing organisms (58). Current evidence suggests that *Geobacter* species directly contact Fe(III) oxides (68), whereas other species, such as *Geothrix* (67) and possibly *Shewanella* (40, 68, 69) species, secrete a quinone-like water-soluble compound that serves as an electron shuttle between the surface of the cell and Fe(III), although this possibility is not without controversy (63).

In order to gain insight into the cost of producing a shuttle, menaquinone was selected as a model shuttling compound. The minimal concentration of electron shuttle that must be
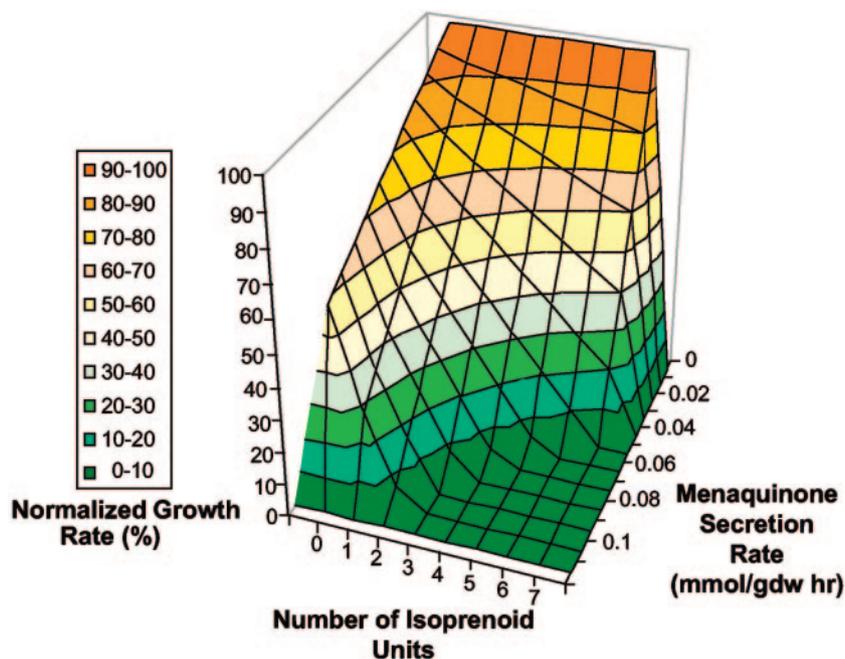
FIG. 4. Analysis of energetic costs associated with secretion of model, electron-shuttling compounds. The growth rate reduction due to the ATP and carbon requirements for menaquinone synthesis is presented. Growth rates are shown as a fraction of the maximum achieved with an acetate uptake rate of 10 mmol/gdw/h and Fe(III)-citrate provided as the electron acceptor.

maintained to be effective was assumed to be 2 μM (49). In subsurface environments shuttles released extracellularly will be lost via diffusion and advection. A very conservative estimate of the rate of this loss is 1% per hour. At cell densities on the order of 10^6 per ml, a secretion rate of 0.02 mmol/gdw/h would be required to maintain minimal shuttle concentrations. Even with these conservative estimates and assuming a typical acetate consumption rate of 0.01 mmol/liter/h, synthesis of the quinone group of menaquinone reduced the growth rate by 9% (Fig. 4). As the size of the menaquinone molecule was increased with the addition of progressively larger side chains, the growth rate decreased by as much as 40% for the largest shuttling molecule considered.

These results suggest that the energy cost associated with synthesizing a secreted compound for electron shuttling can lead to significant reductions in biomass yields for an acetate-oxidizing organism. However, it is important to note that this analysis was done with the menaquinone as a representative compound and that additional analyses will be required to assess the biosynthetic demands associated with the production of actual electron shuttles once their structures and secretion rates are determined.

Functional analysis of *G. sulfurreducens* mutant phenotypes. The availability of a genome scale model also enabled the characterization of systems level properties of the metabolic network. One such property is the set of genes and reactions that are essential to support growth in a defined medium. This information is important for genetic investigations since it can provide insight into which mutations may or may not have an observable phenotype.

In silico deletion analysis (26) for growth with acetate as the electron donor and Fe(III)-citrate or fumarate as the electron acceptor indicated that most mutations were predicted to have either lethal [139 for fumarate and 143 for Fe(III)] or silent [440 for fumarate and 437 for Fe(III)] phenotypes (Fig. 5 and Table S4 in the supplemental material). Lethal mutations (e.g., deletion of acetyl-CoA transferase and pyruvate carboxylase) reflected the inability of the perturbed network to synthesize essential components from acetate, a relatively simple two-carbon compound, or the fact that a nonfermentable substrate such as acetate presents few alternative energy-yielding oxidative mechanisms.

Some silent phenotypes predicted by this analysis corresponded to reactions associated with seemingly redundant enzymes. The presence of functionally similar (but nonorthologous) enzymes could be due to selection for genetic robustness, in order to protect against mutations in essential reactions. Alternatively, this redundancy could reflect a need for metabolic robustness, in which different enzymes are needed to favor flux in opposite directions or are optimized for oxidation of different substrates. For instance, model simulations indicated that a mutation in any component of pyruvate-ferredoxin oxidoreductase would be compensated for by activity of pyruvate dehydrogenase or pyruvate-formate-lyase. However, since pyruvate-formate-lyase strongly favors function in the oxidative direction, it is unlikely that this enzyme can substitute for pyruvate-ferredoxin oxidoreductase in vivo, and the redundancy at this node likely reflects the presence of enzymes specialized for different tasks. Mutational and biochemical investigations are under way to test these hypotheses.

Large-scale in silico deletion analysis identified only 17 reactions (of 522 [3.25%]) that when deleted would be nonlethal but would have an effect on growth rate during acetate-limited growth (acetate uptake of 5 mmol/gdw/h) with fumarate as the
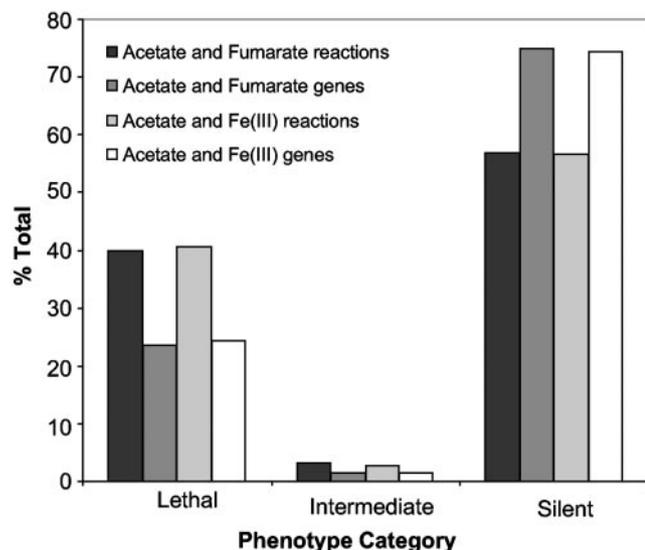
FIG. 5. Impact of in silico deletion of single genes, or entire reactions, on predicted growth rate of *G. sulfurreducens*. The impact of all possible single-gene ($n = 588$) and reaction ($n = 522$) deletions were analyzed. A histogram of the percentage of deletions resulting in no growth (lethal), a growth rate greater than zero but less than that of the wild type (intermediate), and wild-type growth rate (silent) is shown for both fumarate- and Fe(III)-reducing conditions. The acetate uptake rate was constrained to 10 mmol/gdw/h for Fe(III) citrate reduction and to 5 mmol/gdw/h for fumarate reduction. In both cases, acetate was the limiting nutrient.
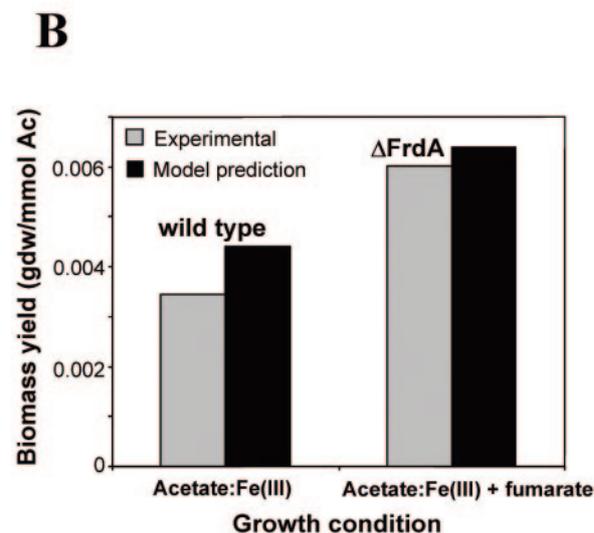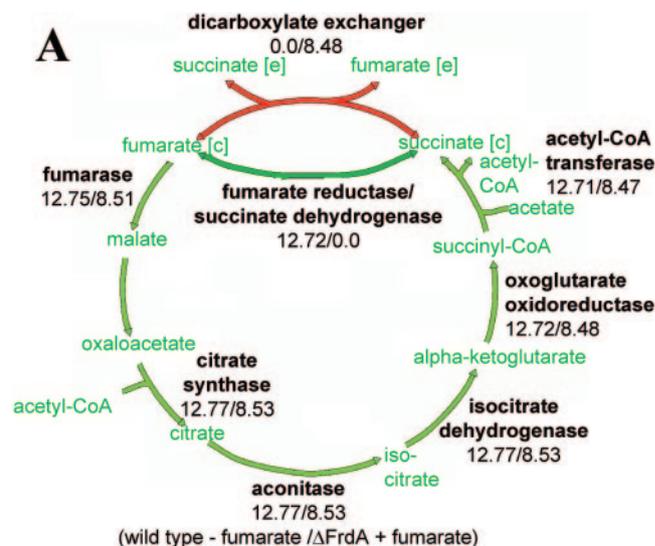

FIG. 6. In silico phenotypic analysis of the fumarate reductase/ succinate dehydrogenase knockout strain (ΔFrdA). (A) Comparison of predicted central metabolic flux distributions in the wild-type strain growing in unsupplemented acetate-Fe(III) citrate to those of the knockout strain growing in acetate (4.88 mM)-Fe(III) citrate (30 mM) medium supplemented with 10 mM fumarate. Predicted fluxes (wild type/ΔFrdA, mmol/gdw/h) are indicated below enzyme names. Red arrows indicate significant flux only in the fumarate supplemented mutant strain. Dark green arrows indicate flux present only in the wild-type strain. In the cases of fumarate and succinate, "[e]" denotes extracellular, whereas "[c]" denotes cytoplasmic. (B) Comparison of predicted and experimental biomass yields for the wild type and the ΔFrdA strain. Cells were grown in chemostats in the presence of limiting acetate at a dilution rate of 0.06 h^{-1}. Model simulations of acetate-limited growth were carried out by constraining growth rate at 0.06 h^{-1} and minimizing the acetate uptake rate.

acceptor. In contrast, in silico deletion of 59 reactions (6.4% of total) in the *E. coli* network resulted in an intermediate growth rate during glucose-limited aerobic growth (79). The lack of many intermediate modes of growth again reflects the fact that *G. sulfurreducens* utilizes electron donors (acetate) and acceptors that cannot be metabolized by alternative pathways such as partial oxidation, fermentation, or routing of metabolites through pathways that would consume ATP, which is already in short supply.

Because of its importance to the energetics and TCA cycle function of *Geobacter*, the mutant phenotype resulting from deletion of the bifunctional succinate dehydrogenase-fumarate reductase (FrdA) was investigated further. Since a mutant in the catalytic subunit for this enzyme already has been characterized, it was possible to compare in silico and in vivo phenotypes (11). The model correctly predicted that the FrdA-deficient mutant would be unable to reduce fumarate and would be unable to grow with Fe(III)-citrate as the electron acceptor and acetate as the electron donor, since cells lacking the succinate dehydrogenase would be unable to complete the TCA cycle. Likewise, the model predicted that the mutant could grow with Fe(III)-citrate as the electron acceptor and H$_2$ as the electron donor, if acetate was provided as a carbon source. In fact, this was the condition under which the FrdA-deficient strain was recovered.

The FrdA-deficient strain was previously reported to grow by oxidizing acetate with Fe(III)-citrate as the electron acceptor if the medium was supplemented with fumarate to allow completion of the TCA cycle (11). When "rescuing" the TCA cycle in this manner, the FrdA-deficient strain grew at a faster rate and obtained higher yields than those of the wild-type strain growing in unsupplemented medium. In model simulations, an identical phenotype was observed (Fig. 6). In this case, fumarate was not used as a carbon or energy source since *G. sulfurreducens* can utilize fumarate only in the fumarate reductase due to the requirement for equimolar exchange of fumarate and succinate. Thus, the increase in growth yield for

the fumarate-supplemented mutant was found to be due to the elimination of the energy cost associated with the cytosolic protons produced during succinate oxidation under Fe(III)-reducing conditions.

To further evaluate this phenotype, steady-state growth experiments in chemostats were conducted that confirmed the magnitude of the growth yield increase predicted in silico (Fig. 6). The individual flux predictions for each TCA cycle reaction illustrate how the wild-type cells, which achieved a lower ATP yield per acetate oxidized, respired more rapidly to maintain the same growth rate as the fumarate-supplemented mutant. These results demonstrated the ability of the in silico model to make quantitative predictions and further highlight the energetic impact of cytosolic proton production during Fe(III) reduction by *G. sulfurreducens*.

Conclusions. The results presented here demonstrate that genome-scale metabolic modeling can enhance physiological studies of environmentally relevant microorganisms. Most previous models of microbial metabolism have been developed for microorganisms such as *E. coli*, for which there was already substantial physiological information. The model for *G. sulfurreducens* is the first integrated genome-scale model available for an organism that is capable of the complete anaerobic oxidation of organic compounds via the TCA cycle and respiration with metals. The importance of a completely balanced system-wide model of metabolism revealed the importance of cytosolic proton production and its energetic implications and was critical for elucidating previously unexplained lower cell yields during growth with Fe(III) as the electron acceptor. The model has played a critical role in the initial functional analysis of the *G. sulfurreducens* genome and has generated testable hypotheses regarding strategies for Fe(III) reduction, carbon assimilation, and energy production. The availability of the model can enhance the characterization of metabolism in different environments when alternative donors such as pyruvate, formate, and hydrogen are present. As investigators become more adept at isolating environmentally relevant organisms (17, 42, 78, 81, 90) and the cost and time required to sequence microbial genomes decreases, the development of genome-scale models coupled with the appropriate experimentation might accelerate understanding of other uncharacterized but environmentally relevant microorganisms.

ACKNOWLEDGMENTS

REFERENCES

1. **Altschul, S. F., T. L. Madden, A. A. Schaffer, J. Zhang, Z. Zhang, W. Miller, and D. J. Lipman.** 1997. Gapped BLAST and PSI-BLAST: a new generation of protein database search programs. Nucleic Acids Res. **25:**3389–3402.
2. **Anderson, R. T., J. N. Rooney-Varga, C. V. Gaw, and D. R. Lovley.** 1998. Anaerobic benzene oxidation in the Fe(III) reduction zone of petroleum contaminated aquifers. Environ. Sci. Technol. **32:**1222–1229.
3. **Anderson, R. T., H. A. Vrionis, I. Ortiz-Bernad, C. T. Resch, P. E. Long, R. Dayvault, K. Karp, S. Marutzky, D. R. Metzler, A. Peacock, D. C. White, M. Lowe, and D. R. Lovley.** 2003. Stimulating the in situ activity of *Geobacter* species to remove uranium from the groundwater of a uranium-contaminated aquifer. Appl. Environ. Microbiol. **69:**5884–5891.
4. **Ashwell, G.** 1957. Estimation of total carbohydrate in solution, in suspension, or in whole cells or tissue by the anthrone method. Methods Enzymol. **3:**73–78.
5. **Beard, D. A., S. C. Liang, and H. Qian.** 2002. Energy balance for analysis of complex metabolic networks. Biophys. J. **83:**79–86.
6. **Biel, S., J. Simon, R. Gross, T. Ruiz, M. Ruitenberg, and A. Kroger.** 2002. Reconstitution of coupled fumarate respiration in liposomes by incorporating the electron transport enzymes isolated from *Wolinella succinogenes*. Eur. J. Biochem. **269:**1974–1983.
7. **Bonarius, H. P. J., G. Schmid, and J. Tramper.** 1997. Flux analysis of underdetermined metabolic networks: the quest for the missing constraints. Trends Biotechnol. **15:**308–314.
8. **Bond, D. R., D. E. Holmes, L. M. Tender, and D. R. Lovley.** 2002. Electrode-reducing microorganisms that harvest energy from marine sediments. Science **295:**483–485.
9. **Bond, D. R., and D. R. Lovley.** 2003. Electricity production by *Geobacter sulfurreducens* attached to electrodes. Appl. Environ. Microbiol. **69:**1548–1555.
10. **Burgard, A. P., E. V. Nikolaev, C. H. Schilling, and C. D. Maranas.** 2004. Flux coupling analysis of genome-scale metabolic network reconstructions. Genome Res. **14:**301–312.
11. **Butler, J. E., R. H. Glaven, A. Esteve-Nunez, C. Nunez, E. S. Shelobolina, D. R. Bond, and D. R. Lovley.** 2006. Genetic characterization of a single bifunctional enzyme for fumarate reduction and succinate oxidation in *Geobacter sulfurreducens* and engineering of fumarate reduction in *Geobacter metallireducens*. J. Bacteriol. **188:**450–455.
12. **Caccavo, F., Jr., D. J. Lonergan, D. R. Lovley, M. Davis, J. F. Stolz, and M. J. McInerney.** 1994. *Geobacter sulfurreducens* sp. nov., a hydrogen- and acetate-oxidizing dissimilatory metal-reducing microorganism. Appl. Environ. Microbiol. **60:**3752–3759.
13. **Champine, J. E., and S. Goodwin.** 1991. Acetate catabolism in the dissimilatory iron-reducing isolate GS-15. J. Bacteriol. **173:**2704–2706.
14. **Champine, J. E., B. Underhill, J. M. Johnston, W. W. Lilly, and S. Goodwin.** 2000. Electron transfer in the dissimilatory iron-reducing bacterium *Geobacter metallireducens*. Anaerobe **6:**187–196.
15. **Childers, S. E., S. Ciufo, and D. R. Lovley.** 2002. *Geobacter metallireducens* accesses insoluble Fe(III) oxide by chemotaxis. Nature **416:**767–769.
16. **Chvatal, V.** 1983. Linear programming. W. H. Freeman, New York, N.Y.
17. **Connon, S. A., and S. J. Giovannoni.** 2002. High-throughput methods for culturing microorganisms in very-low-nutrient media yield diverse new marine isolates. Appl. Environ. Microbiol. **68:**3878–3885.
18. **Coppi, M. V., C. Leang, F. Kaufmann, R. A. O'Neil, D. R. Bond, and D. R. Lovley.** Genetic analysis of a putative soluble Fe(III) reductase from *Geobacter sulfurreducens*. Submitted for publication.
19. **Coppi, M. V., R. A. O'Neil, and D. R. Lovley.** 2004. Identification of an uptake hydrogenase required for hydrogen-dependent reduction of Fe(III) and other electron acceptors by *Geobacter sulfurreducens*. J. Bacteriol. **186:** 3022–3028.
20. **Cord-Ruwisch, R., D. R. Lovley, and B. Schink.** 1998. Growth of *Geobacter sulfurreducens* with acetate in syntrophic cooperation with hydrogen-oxidizing anaerobic partners. Appl. Environ. Microbiol. **64:**2232–2236.
21. **Covert, M. W., C. H. Schilling, I. Famili, J. S. Edwards, I. I. Goryanin, E. Selkov, and B. O. Palsson.** 2001. Metabolic modeling of microbial strains in silico. Trends Biochem. Sci. **26:**179–186.
22. **Cronan, J. E., and D. Laporte.** 1996. Tricarboxylic acid cycle and glyoxalate bypass, p. 189–198. *In* F. C. Neidhardt, R. Curtiss III, J. L. Ingraham, E. C. C. Lin, K. B. Low, B. Magasanik, W. S. Reznikoff, M. Riley, M. Schaechter, and H. E. Umbarger (ed.), *Escherichia coli* and *Salmonella*: cellular and molecular biology, 2nd ed. ASM Press, Washington, D.C.
23. **Daae, E. B., and A. P. Ison.** 1999. Classification and sensitivity analysis of a proposed primary metabolic reaction network for *Streptomyces lividans*. Metab. Eng. **1:**153–165.
24. **Duarte, N. C., M. J. Herrgard, and B. Palsson.** 2004. Reconstruction and validation of *Saccharomyces cerevisiae* iND750, a fully compartmentalized genome-scale metabolic model. Genome Res. **14:**1298–1309.
25. **Edwards, J. S., and B. O. Palsson.** 1999. Systems properties of the *Haemophilus influenzae* Rd metabolic genotype. J. Biol. Chem. **274:**17410–17416.
26. **Edwards, J. S., and B. O. Palsson.** 2000. Metabolic flux balance analysis and the in silico analysis of *Escherichia coli* K-12 gene deletions. BMC Bioinformatics **1:**1.
27. **Edwards, J. S., and B. O. Palsson.** 2000. The *Escherichia coli* MG1655 in silico metabolic genotype: its definition, characteristics, and capabilities. Proc. Natl. Acad. Sci. USA **97:**5528–5533.
28. **Esteve-Nunez, A., C. Nunez, and D. R. Lovley.** 2004. Preferential reduction of Fe(III) over fumarate by *Geobacter sulfurreducens*. J. Bacteriol. **186:**2897–2899.
29. **Esteve-Nunez, A., A. Rothermich, M. Sharma, and D. R. Lovley.** 2005. Growth of *Geobacter sulfurreducens* under nutrient-limiting conditions in continuous culture. Environ. Microbiol. **7:**641–648.
30. **Famili, I., J. Forster, J. Nielsen, and B. O. Palsson.** 2003. *Saccharomyces cerevisiae* phenotypes can be predicted by using constraint-based analysis of a genome-scale reconstructed metabolic network. Proc. Natl. Acad. Sci. USA **100:**13134–13139.
31. **Fernandes, A. S., A. A. Konstantinov, M. Teixeira, and M. M. Pereira.** 2005. Quinone reduction by *Rhodothermus marinus* succinate:menaquinone oxi-

doreductase is not stimulated by the membrane potential. Biochem. Biophys. Res. Commun. **330:**565–570.

32. **Folch, J., M. Lees, and G. Sloane-Stanley.** 1957. A simple method for the isolation and purification of total lipids from animal tissues. J. Biol. Chem. **226:**497–509.

33. **Friedrich, T., and D. Scheide.** 2000. The respiratory complex I of bacteria, archaea, and eukarya and its module common with membrane-bound multisubunit hydrogenases. FEBS Lett. **479:**1–5.

34. **Galushko, A. S., and B. Schink.** 2000. Oxidation of acetate through reactions of the citric acid cycle by *Geobacter sulfurreducens* in pure culture and in syntrophic coculture. Arch. Microbiol. **174:**314–321.

35. **Gebhardt, N. A., R. K. Thauer, D. Linder, P. M. Kaulfers, and N. Pfennig.** 1985. Mechanism of acetate oxidation to carbon dioxide with elemental sulfur in *Desulfuromonas acetoxidans.* Arch. Microbiol. **141:**392–398.

36. **Geisler, V., R. Ullmann, and A. Kroger.** 1994. The direction of the proton-exchange associated with the redox reactions of menaquinone during electron-transport in *Wolinella succinogenes.* Biochim. Biophys. Acta-Bioenergetics **1184:**219–226.

37. **Goto, S., Y. Okuno, M. Hattori, T. Nishioka, and M. Kanehisa.** 2002. LIGAND: database of chemical compounds and reactions in biological pathways. Nucleic Acids Res. **30:**402–404.

38. **Hagerhall, C., and L. Hederstedt.** 1996. A structural model for the membrane-integral domain of succinate:quinone oxidoreductases. FEBS Lett. **389:**25–31.

39. **Herbert, D., P. J. Phipps, and R. E. Strange.** 1971. Chemical analysis of microbial cells. Methods Enzymol. **5B:**210–234.

40. **Hernandez, M. E., and D. K. Newman.** 2001. Extracellular electron transfer. Cell. Mol. Life Sci. **58:**1562–1571.

41. **Holmes, D. E., K. T. Finneran, R. A. O'Neil, and D. R. Lovley.** 2002. Enrichment of members of the family *Geobacteraceae* associated with stimulation of dissimilatory metal reduction in uranium-contaminated aquifer sediments. Appl. Environ. Microbiol. **68:**2300–2306.

42. **Kaeberlein, T., K. Lewis, and S. S. Epstein.** 2002. Isolating "uncultivable" microorganisms in pure culture in a simulated natural environment. Science **296:**1127–1129.

43. **Kanehisa, M., S. Goto, S. Kawashima, Y. Okuno, and M. Hattori.** 2004. The KEGG resource for deciphering the genome. Nucleic Acids Res. **32**(database issue):D277–D280.

44. **Kauffman, K. J., P. Prakash, and J. S. Edwards.** 2003. Advances in flux balance analysis. Curr. Opin. Biotechnol. **14:**491–496.

45. **Kroger, A., V. Geisler, E. Lemma, F. Theis, and R. Lenger.** 1992. Bacterial fumarate respiration. Arch. Microbiol. **158:**311–314.

46. **Lee, S., C. Phalakornkule, M. M. Domach, and I. E. Grossmann.** 2000. Recursive MILP model for finding all the alternate optima in LP models for metabolic networks. Comput. Chem. Eng. **24:**711–716.

47. **Lehninger, A. L., M. M. Cox, and D. L. Nelson.** 1993. Principles of biochemistry. Worth Publishers, New York, N.Y.

48. **Lin, W. C., M. V. Coppi, and D. R. Lovley.** 2004. *Geobacter sulfurreducens* can grow with oxygen as a terminal electron acceptor. Appl. Environ. Microbiol. **70:**2525–2528.

49. **Lloyd, J. R., E. L. Blunt-Harris, and D. R. Lovley.** 1999. The periplasmic 9.6-kilodalton c-type cytochrome of *Geobacter sulfurreducens* is not an electron shuttle to Fe(III). J. Bacteriol. **181:**7647–7649.

50. **Lloyd, J. R., C. Leang, A. L. Hodges-Myerson, M. V. Coppi, S. Cuifo, B. Methe, S. J. Sandler, and D. R. Lovley.** 2003. Biochemical and genetic characterization of PpcA, a periplasmic c-type cytochrome in *Geobacter sulfurreducens.* Biochem. J. **369:**153–161.

51. **Lloyd, J. R., and L. E. Macaskie.** 2000. Bioremediation of radioactive metals, p. 272–327. *In* D. R. Lovley (ed.), Environmental microbe-metal interactions. ASM Press, Washington, D.C.

52. **Lloyd, J. R., V. A. Sole, C. V. Van Praagh, and D. R. Lovley.** 2000. Direct and Fe(II)-mediated reduction of technetium by Fe(III)-reducing bacteria. Appl. Environ. Microbiol. **66:**3743–3749.

53. **Lovley, D. R.** 1991. Dissimilatory Fe(III) and Mn(IV) reduction. Microbiol. Rev. **55:**259–287.

54. **Lovley, D. R.** 2003. Cleaning up with genomics: applying molecular biology to bioremediation. Nat. Rev. Microbiol. **1:**35–44.

55. **Lovley, D. R., and R. T. Anderson.** 2000. Influence of dissimilatory metal reduction on the fate of organic and metal contaminants in the subsurface. Hydogeol. J. **8:**77–88.

56. **Lovley, D. R., M. Baedecker, D. J. Lonergan, I. Cozzarelli, E. J. P. Phillips, and D. Siegel.** 1989. Oxidation of aromatic contaminants coupled to microbial iron reduction. Nature **339:**297–300.

57. **Lovley, D. R., S. J. Giovannoni, D. C. White, J. E. Champine, E. J. Phillips, Y. A. Gorby, and S. Goodwin.** 1993. *Geobacter metallireducens* gen. nov. sp. nov., a microorganism capable of coupling the complete oxidation of organic compounds to the reduction of iron and other metals. Arch. Microbiol. **159:**336–344.

58. **Lovley, D. R., D. E. Holmes, and K. P. Nevin.** 2004. Dissimilatory Fe(III) and Mn(IV) reduction. Adv. Microb. Physiol. **49:**219–286.

59. **Lovley, D. R., E. J. P. Phillips, Y. A. Gorby, and E. R. Landa.** 1991. Microbial reduction of uranium. Nature **350:**413–416.

60. **Magnuson, T. S., A. L. Hodges-Myerson, and D. R. Lovley.** 2000. Characterization of a membrane-bound NADH-dependent Fe³⁺ reductase from the dissimilatory Fe³⁺-reducing bacterium *Geobacter sulfurreducens.* FEMS Microbiol. Lett. **185:**205–211.

61. **Mahadevan, R., and C. H. Schilling.** 2003. The effects of alternate optimal solutions in constraint-based genome-scale metabolic models. Metab. Eng. **5:**264–276.

62. **Methe, B. A., K. E. Nelson, J. A. Eisen, I. T. Paulsen, W. Nelson, J. F. Heidelberg, D. Wu, M. Wu, N. Ward, M. J. Beanan, R. J. Dodson, R. Madupu, L. M. Brinkac, S. C. Daugherty, R. T. Deboy, A. S. Durkin, M. Gwinn, J. F. Kolonay, S. A. Sullivan, D. H. Haft, J. Selengut, T. M. Davidsen, N. Zafar, O. White, B. Tran, C. Romero, H. A. Forberger, J. Weidman, H. Khouri, T. V. Feldblyum, T. R. Utterback, S. E. Van Aken, D. R. Lovley, and C. M. Fraser.** 2003. Genome of *Geobacter sulfurreducens*: metal reduction in subsurface environments. Science **302:**1967–1969.

63. **Myers, C. R., and J. A. Myers.** 2004. *Shewanella oneidensis* MR-1 restores menaquinone synthesis to a menaquinone-negative mutant. Appl. Environ. Microbiol. **70:**5415–5425.

64. **Neidhardt, F., J. L. Ingraham, and M. Shaechter.** 1990. Physiology of the bacterial cell. Sinauer Associates, Inc., Sunderland, MA.

65. **Neidhardt, F., and H. E. Umbarger.** 1996. Chemical composition of *Escherichia coli*, p. 13–16. *In* F. C. Neidhardt, R. Curtiss III, J. L. Ingraham, E. C. C. Lin, K. B. Low, B. Magasanik, W. S. Reznikoff, M. Riley, M. Schaechter, and H. E. Umbarger (ed.), *Escherichia coli* and *Salmonella*: cellular and molecular biology, 2nd ed. ASM Press, Washington, D.C.

66. **Neijssel, O. M., M. J. Teixeria de Mattos, and D. W. Tempest.** 1996. Growth yield and energy distribution, p. 1683–1692. *In* F. C. Neidhardt, R. Curtiss III, J. L. Ingraham, E. C. C. Lin, K. B. Low, B. Magasanik, W. S. Reznikoff, M. Riley, M. Schaechter, and H. E. Umbarger (ed.), *Escherichia coli* and *Salmonella*: cellular and molecular biology, 2nd ed. ASM Press, Washington, D.C.

67. **Nevin, K. P., and D. R. Lovley.** 2002. Mechanisms for accessing insoluble Fe(III) oxide during dissimilatory Fe(III) reduction by *Geothrix fermentans.* Appl. Environ. Microbiol. **68:**2294–2299.

68. **Nevin, K. P., and D. R. Lovley.** 2002. Mechanisms for Fe(III) oxide reduction in sedimentary environments. Geomicrobiol. J. **19:**141–159.

69. **Newman, D. K., and R. Kolter.** 2000. A role for excreted quinones in extracellular electron transfer. Nature **405:**94–97.

70. **Ortiz-Bernad, I., R. T. Anderson, H. A. Vrionis, and D. R. Lovley.** 2004. Vanadium respiration by *Geobacter metallireducens*: novel strategy for in situ removal of vanadium from groundwater. Appl. Environ. Microbiol. **70:**3091–3095.

71. **Overbeek, R., N. Larsen, G. D. Pusch, M. D'Souza, E. Selkov, Jr., N. Kyrpides, M. Fonstein, N. Maltsev, and E. Selkov.** 2000. WIT: integrated system for high-throughput genome sequence analysis and metabolic reconstruction. Nucleic Acids Res. **28:**123–125.

72. **Paulsen, J., A. Kroger, and R. K. Thauer.** 1986. ATP driven succinate oxidation in the catabolism of *Desulfuromonas acetoxidans.* Arch. Microbiol. **144:**78–83.

73. **Pirt, S. J.** 1965. The maintenance energy of bacteria in growing cultures. Proc. R. Soc. London **163:**224–231.

74. **Pramanik, J., and J. D. Keasling.** 1997. Stoichiometric model of *Escherichia coli* metabolism: incorporation of growth-rate dependent biomass composition and mechanistic energy requirements. Biotechnol. Bioeng. **56:**398–421.

75. **Pramanik, J., and J. D. Keasling.** 1998. Effect of *Escherichia coli* biomass composition on central metabolic fluxes predicted by a stoichiometric model. Biotechnol. Bioeng. **60:**230–238.

76. **Price, N. D., I. Famili, D. A. Beard, and B. O. Palsson.** 2002. Extreme pathways and Kirchhoff's second law. Biophys. J. **83:**2879–2882.

77. **Price, N. D., J. A. Papin, C. H. Schilling, and B. Palsson.** 2003. Genome-scale microbial in silico models: the constraints-based approach. Trends Biotechnol. **21:**162–169.

78. **Rappe, M. S., S. A. Connon, K. L. Vergin, and S. J. Giovannoni.** 2002. Cultivation of the ubiquitous SAR11 marine bacterioplankton clade. Nature **418:**630–633.

79. **Reed, J. L., T. D. Vo, C. H. Schilling, and B. Palsson.** 2003. *Escherichia coli* iJR904: an expanded genome-scale model of *E. coli* K-12. Genome Biol. **4:**R54.1–R54.12.

80. **Reguera, G., K. D. McCarthy, T. Mehta, J. S. Nicoll, M. T. Tuominen, and D. R. Lovley.** 2005. Extracellular electron transfer via microbial nanowires. Nature **435:**1098–1101.

81. **Sait, M., P. Hugenholtz, and P. H. Janssen.** 2002. Cultivation of globally distributed soil bacteria from phylogenetic lineages previously only detected in cultivation-independent surveys. Environ. Microbiol. **4:**654–666.

82. **Schilling, C. H., M. W. Covert, I. Famili, G. M. Church, J. S. Edwards, and B. O. Palsson.** 2002. Genome-scale metabolic model of *Helicobacter pylori* 26695. J. Bacteriol. **184:**4582–4593.

83. **Schneider, W. C.** 1957. Determination of nucleic acids in tissues. Methods Enzymol. **3:**680–684.

84. **Schnorpfeil, M., I. G. Janausch, S. Biel, A. Kroger, and G. Unden.** 2001. Generation of a proton potential by succinate dehydrogenase of *Bacillus subtilis* functioning as a fumarate reductase. Eur. J. Biochem. **268:**3069–3074.

85. **Smith, P. K., R. I. Krohn, G. T. Hermanson, A. K. Mallia, F. H. Gartner, M. D. Provenzano, E. K. Fujimoto, N. M. Goeke, B. J. Olson, and D. C. Klenk.** 1985. Measurement of protein using bicinchoninic acid. Anal. Biochem. **150:**76–85.

86. **Ullmann, R., R. Gross, J. Simon, G. Unden, and A. Kroger.** 2000. Transport of C(4)-dicarboxylates in *Wolinella succinogenes*. J. Bacteriol. **182:** 5757–5764.

87. **Varma, A., and B. Palsson.** 1994. Metabolic flux balancing: basic concepts, scientific and practical use. Bio/Technology **12:**994–998.

88. **Weiner, J. M., and D. R. Lovley.** 1998. Anaerobic benzene degradation in petroleum-contaminated aquifer sediments after inoculation with a benzene-oxidizing enrichment. Appl. Environ. Microbiol. **64:**775–778.

89. **Yagi, T., and A. Matsuno-Yagi.** 2003. The proton-translocating NADH-quinone oxidoreductase in the respiratory chain: the secret unlocked. Biochemistry **42:**2266–2274.

90. **Zengler, K., G. Toledo, M. Rappe, J. Elkins, E. J. Mathur, J. M. Short, and M. Keller.** 2002. Cultivating the uncultured. Proc. Natl. Acad. Sci. USA **99:**15681–15686.

91. **Zhu, G., G. B. Golding, and A. M. Dean.** 2005. The selective cause of an ancient adaptation. Science **307:**1279–1282.